J Therm Anal Calorim (2012) 110:573–580
DOI 10.1007/s10973-012-2728-1

Thermal, structural, magnetic and photoluminescence studies on cobalt ferrite nanoparticles obtained by citrate precursor method

R. K. Singh · A. Narayan · K. Prasad · R. S. Yadav · A. C. Pandey · A. K. Singh · L. Verma · R. K. Verma

Received: 20 August 2012 / Accepted: 21 September 2012 / Published online: 11 October 2012

Abstract Magnetic nanoparticles of cobalt ferrite have been synthesized by citrate precursor method. TG-DSC studies have been made to get the idea of the optimum temperature of annealing that could lead to the formation of nanoparticles. Annealing the citrate precursor was done at 450, 650, and 973 °C. The X-ray diffraction (XRD) studies and the scanning electron microscopy (SEM) have been used for characterization. The data from vibrating sample magnetometer and photoluminescence spectrometer (PL) have been analyzed for exploring their applications. Using the Scherrer formula, the crystallite size was found to be 25, 32, and 43 nm, respectively, using the three temperatures. The particle size increased with annealing temperature. Rietveld refinements on the X-ray (XRD) data were done on the cobalt ferrite nanoparticles (monoclinic cells) obtained on annealing at 650 °C, selecting the space group P2/M. The values of coercivity (1574.4 G) and retentivity (18.705 emu g^{-1}) were found out in the sample annealed at 650 °C while magnetization (39.032 emu g^{-1}) was also found in the sample annealed at 973 °C. The photoluminescence (PL) property of these samples were studied using 225, 330, and 350 nm excitation wavelength radiation source. The PL intensity was found to be increasing with the particle size.

Keywords TG-DSC studies · Dehydrated gel · Cobalt ferrite · Nanoparticles · Spinel · Rietveld analysis · Coercivity · Magnetization · Thermal stability · Photoluminescence

R. K. Singh
Department of Physics, Patna Women's College, Patna 800 001, India

A. Narayan
P.G. Department of Physics, Patna University, Patna 800 005, India

K. Prasad
Department of Physics, Central University of Jharkhand, Ranchi 835205, India

R. S. Yadav · A. C. Pandey
Nanotechnology Application Centre, University of Allahabad, Allahabad 211002, India

A. K. Singh · L. Verma · R. K. Verma (✉)
Thermal Analysis Lab, University Department of Chemistry, Magadh University, Bodh-Gaya 824234, India
e-mail: profrkverma@gmail.com

Introduction

The last few decades have witnessed exponential growth in the applications of commercial electronics following discovery of certain very useful materials. A typical example is cobalt ferrite which has gained enormous significance on account of its high electromagnetic performance [1, 2] besides its excellent chemical stability, good mechanical hardness, and wonderfully high positive first order crystalline anisotropy constant [3]. The quest for magnetic nanoparticles that could be used for high density magnetic recording sensors etc., has attracted many workers toward the cubic spinel-structured cobalt ferrite of variable particle size in which Co^{2+} and Fe^{3+} occupy tetrahedral/octahedral sites in the fcc lattice of O^{2-} ions [1, 4]. The properties of such materials (hence, their applications) as well as their particle size have been found to be greatly depending upon the method of preparation and the annealing/sintering temperature [5–11]. Out of the many synthetic techniques, the sol–gel methods have been found to be effective in getting homogeneous nanoparticles at relatively low temperature [9–11].

Thermogravimetric and DSC data and their kinetic and mechanistic analysis are frequently used to understand the thermal stability of materials and also to study the phase changes, thermodynamics and kinetics of various transformations taking place upon heating [12–22]. The two techniques together give good idea of the completion of such steps. Earlier too, these techniques have been applied in case of chromites and aluminates [23, 24] to get an idea of the minimum temperature at which the decomposition steps are complete so that effective annealing could be started. Thus, in order to achieve optimization of the heat treatment conditions to get nanoparticles of cobalt ferrite of significant saturation magnetization (M_s), magneto crystallization anisotropy (K), coercivity (H_c), and retentivity values [25, 26], the citrate precursor method has been tried as in the case of chromites and aluminates. The citrate gel has been subjected to TG-DSC analysis to get idea of the lowest and the optimum temperature of annealing. It is believed that heat treatment leads to condensation reactions of the metal precursor, which leads to the formation of three dimensional inorganic networks [27] involving strong and rigid metal-oxo-metal (M-O-M) bridges which polymerize and often lead to formation of crystalline clusters as upon further heating, the particles come in contact with each other and grow.

While the TG-DSC technique has been employed in the present work for predicting the optimum temperature of annealing, the X-ray diffraction (XRD) studies and the scanning electron microscopy (SEM) have been used for characterization. The data from vibrating sample magnetometer (VSM) and photoluminescence spectrometer (PL) have been analyzed for exploring their applications.

Experimental

Materials

Samples of nano-sized cobalt ferrite powder were prepared by the citrate precursor method. Ferric nitrate and cobalt nitrate (AR) were taken in stoichiometric proportions as the starting materials. Aqueous solutions of these salts were prepared separately by dissolving the respective salts in minimum amount of deionized water while stirring constantly. The two solutions were then mixed together. Aqueous solution of citric acid was prepared in adequate quantity by weight and was added to the mixture of the salt solutions. The mixture was heated at a temperature in the range 60–80 °C for 2 h with continuous stirring. This solution was allowed to cool down to room temperature, and finally, it was dried at 60–65 °C in an oven until it formed a brown color fluffy mass.

Methods

The dehydrated gel was subjected to TG-DSC studies in N_2 atmosphere with heating rate programed at 10 °C min^{-1}. The TGA-DSC curve of the sample was obtained on TG-DSC 1 (Mettler). Scherrer Formula ($D = 0.9\ \lambda/\beta\ Cos\theta$) was used to calculate the particle size [28]. SEM (Model: Quanta 200 MK 2 Series FEI) was used for confirming the crystallite sizes (3000, 5000, 6000, 10000 and 12000 magnifications).

On the basis of the TG-DSC curves, the precursor was annealed at different temperatures to give cobalt ferrite powder that was later proved to be nano-sized particles. The photoluminescence studies were made using 225, 330, and 350 nm excitation wavelength source.

Results and discussion

Thermal analysis

The TG-DSC curves exhibited a clear first step dehydration around 150 °C followed by a sharp *exo* peak which is accompanying the second step. Sample dried below this threshold temperature has a tendency to absorb moisture. The precursor sample, dried at 100 °C was allowed to absorb moisture in air. Its TG-DSC curves were recorded under the same conditions (N_2/10 °C min^{-1}). This was done to get an idea of a minimum temperature for annealing. Dehydration takes place in the first step of the 5-step decomposition taking place up to 450 °C (Fig. 1). After this temperature, only curing is evident and that too in DSC. So this temperature (450 °C) was chosen as the temperature for annealing in an attempt to go for a low temperature annealing to get cobalt ferrite nanoparticles. Annealing was also done at 650 and 973 °C. Increasing the annealing temperature is bound to bring more crystallinity. Thus the samples of the gel were heated at 450, 650, and 973 °C for 1 h in a muffle furnace. As expected, it has been found latter that the crystallite size is increasing with the annealing temperature on account of condensation reactions that may be accompanying heat treatment (Fig. 2).

XRD studies

The formation of nanoparticles (of cobalt ferrite) was checked by XRD technique using an X-ray Diffractometer (Phillips PW1710, Holland) was used [CuK_α radiation $\lambda = 1.5406$ Å between the Bragg angles 25 and 65°]. The XY data (2θ vs. intensity) obtained from this experiment were plotted with the Win PLOTR program which furnished the angular positions of the peaks [29]. The dimensions of the unit cell (*hkl*-values) and space group of

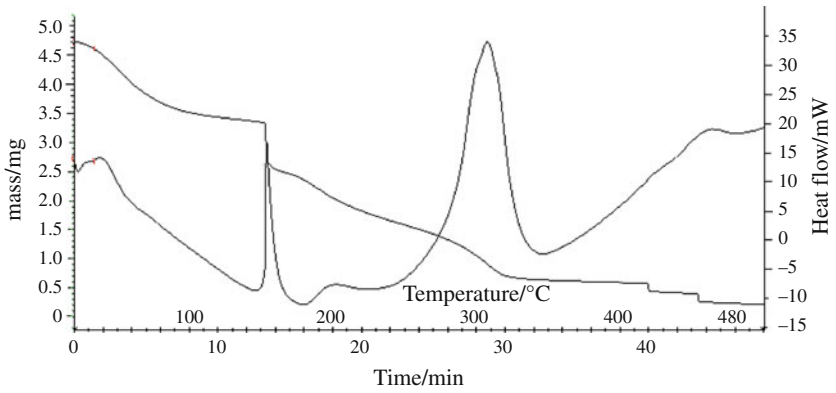

Fig. 1 TG-DSC curves of the rehydrated coprecipitated cobalt(II) citrate-iron citrate gel in N_2 atmosphere

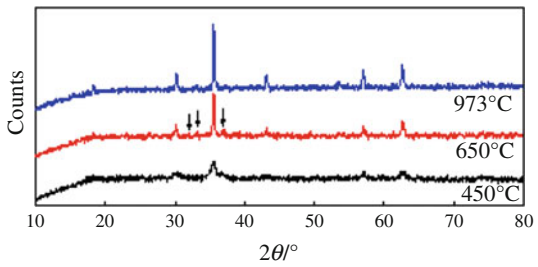

Fig. 2 The XRD curves of the three powder-samples obtained upon annealing at different temperatures

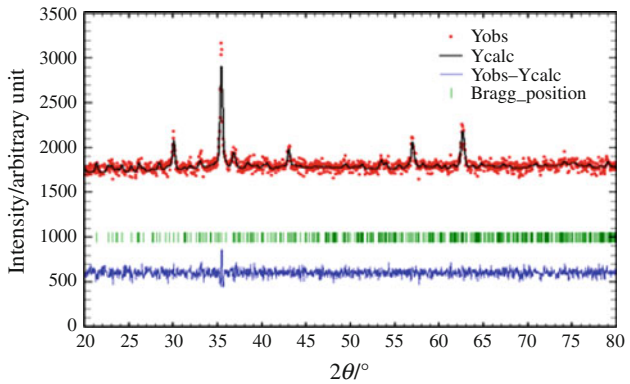

Fig. 3 Rietveld fitting for the sample obtained after annealing at 650 °C

the nanoparticles were obtained using the TREOR program in the FullProf 2000 software package. Refinement was carried out through the profile matching routine of FullProf [30]. The Bragg peaks were modeled with the Pseudo-Voigt function and the background was estimated by linear interpolation between selected background points. The particle size was calculated using the Scherrer formula [24, 28] and was found to be 25, 32, and 43 nm using different annealing temperatures of 450, 650, and 973 °C respectively. The XRD patterns are shown in Fig. 2.

Table 1 The crystal data and refinement factors of $CoFe_2O_4$ nanoparticles (formed upon annealing at 650 °C) as obtained from X-ray powder diffraction data

Parameter	Result	Description of parameter
Crystal System	Monoclinic	
Space group	*P2/M* (10)	
a/Å	7.2960	
b/Å	15.6840	
c/Å	6.0635	
β/°	110.328	
V/Å^3	650.6317	
R_p	109.0	R_p (profile factor) $= 100[\Sigma\|y_i - y_{ic}\|/\Sigma\|y_i\|]$, where y_i is the observed intensity and y_{ic} is the calculated intensity at the ith step.
R_{wp}	58.1	R_{wp} (weighted profile factor) $= 100[\Sigma\omega_i\|y_i\text{-}y_{ic}\|^2/\Sigma\omega_i(y_i)^2]^{1/2}$, where $\omega_i = 1/\sigma_i^2$ and σ_i^2 is variance of the observation.
R_{exp}	44.7	R_{exp} (expected weighted profile factor) $= 100[(n-p)/\Sigma\omega_i(y_i)^2]^{1/2}$, where n and p are the number of profile points and refined parameters, respectively.
R_B	0.924	R_B (Bragg factor) $= 100[\Sigma\|I_{obs} - I_{calc}\|/\Sigma\|I_{obs}\|]$, where I_{obs} is the observed integrated intensity and I_{calc} is the calculated integrated intensity.
R_F	2.98	R_F (crystallographic R_F factor) $= 100[\Sigma\|F_{obs} - F_{calc}\|/\Sigma\|F_{obs}\|]$, where F is the structure factor, $F = \sqrt{(I/L)}$, where L is the Lorentz polarization factor.
χ^2	1.689	$\chi^2 = \Sigma\omega_i(y_i - y_{ic})^2$
d	1.1496	d (Durbin–Watson statistics) $= \Sigma\{[\omega_i(y_i - y_{ic}) - \omega_{i-1}(y_{i-1} - y_{ic-1})]^2\}/\Sigma[\omega_i(y_i - y_{ic})]^2$
Q_D	1.8417	Q_D = expected d
S	1.3	S (goodness of fit) $= (R_{wp}/R_{exp})$

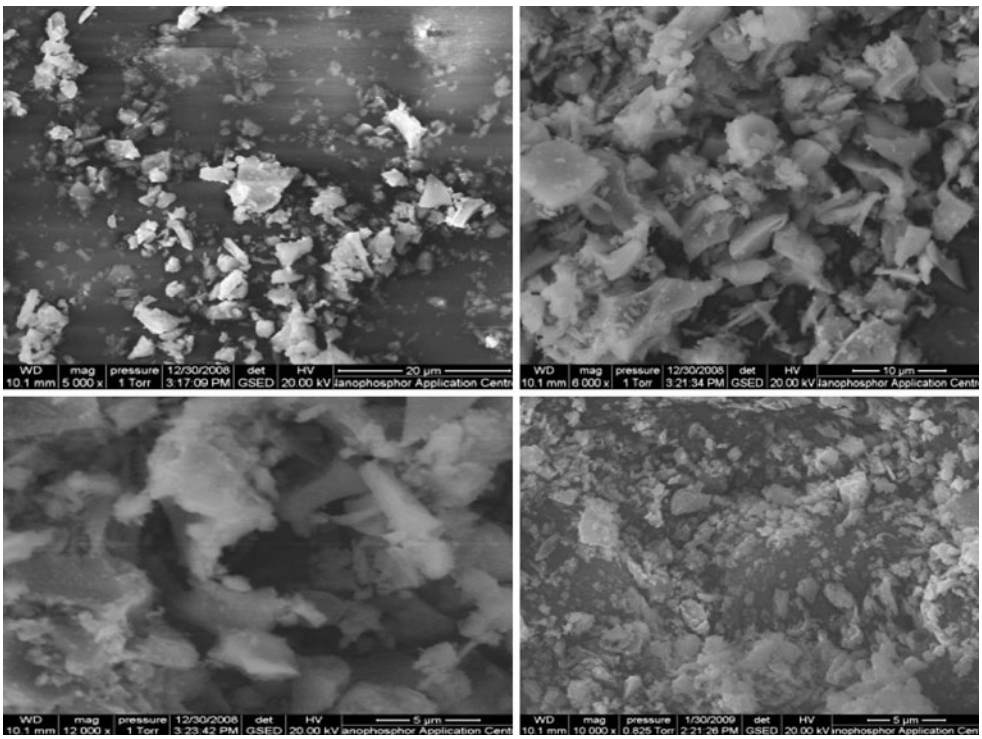

Fig. 4 SEM images of the sample annealed at 450 °C

Rietveld refinements on the X-ray (XRD) data for the sample of the $CoFe_2O_4$ nanoparticles which were obtained after annealing at 650 °C were done selecting the space group *P*2/*M*. Fig. 3 illustrates the observed, calculated, and difference XRD profiles for the nanoparticles after the final cycle of refinement. It can be seen that the profiles for the observed and the calculated one are perfectly matching. The value of χ^2 comes out to be 1.689, which may be considered very good for estimations. The profile fitting procedure adopted was minimizing the χ^2 function [31]. The XRD analyses thus, indicated that the nanoparticle has a monoclinic unit cell. The crystal data and refinement factors as obtained from the XRD data have been presented in Table 1. The lattice constant for sample annealed at 450 °C was 8.356 A and for that at 973 °C was 8.38 A with particle size of 25 and 43 nm, respectively. Normally, a decrease in the particle size results in a decrease of lattice parameters in ferrite nanoparticles, due to change in oxygen co-ordination number with the cations and contribution of excess volume of grain boundaries spin. Attempts have earlier been made to explain the origin of the lattice expansion in the magnetic nanoparticles [32]. Although small, but a systematic shift in XRD peak positions is observed with decrease in particle size.

The Rietveld fitting for sample annealed at 650 °C indicated monoclinic unit cell having a, b, c, β and *V* values of 7.296, 15.684, 6.0635 Å, 110.328(°), and 650.6317 $Å^3$, respectively. Additional Fe_2O_3 phase in sample annealed at 650 °C is distributed in such a way that it is favoring a good hard magnetic material. Super-exchange interaction might have been playing a vital role here.

The particle morphology has been shown in different magnifications (Figs. 4, 5). The SEM analysis of the sample obtained at 650 °C, exhibits formation of individual grains of different shapes as well as few agglomerated grains having different dimensions (0.5–0.8 μm) apart from some submicron-sized grains. The grain size increases with the increase in temperature and the grain growth can clearly be seen at 973 °C.

The ferrite samples were magnetically characterized using VSM. The magnetic parameters obtained from VSM measurements of these samples of Cobalt ferrite particles are tabulated in Table 2 and their magnetic hysteresis curves for the $CoFe_2O_4$ nanoparticles are shown in Fig. 6. The net magnetic moment in the ferrimagnetic materials depends upon the number of magnetic ions occupying the tetrahedral and octahedral sites.

The hysteresis loop for sample annealed at 650 °C shows hard magnetic materials and a decrease in M_s implies existence of the same phases which can diminish or decrease the M_s and the first approximation link goes to existence of some antiferromagnetic phase (Table 2).

Coercivity of $CoFe_2O_4$ nanoparticles could be as high as 4,000 Oe [33] when prepared using chemical route and annealed. The coercivity of the moderate ferrite lies within the range of 100–1,500 Oe, which is suitable for most of

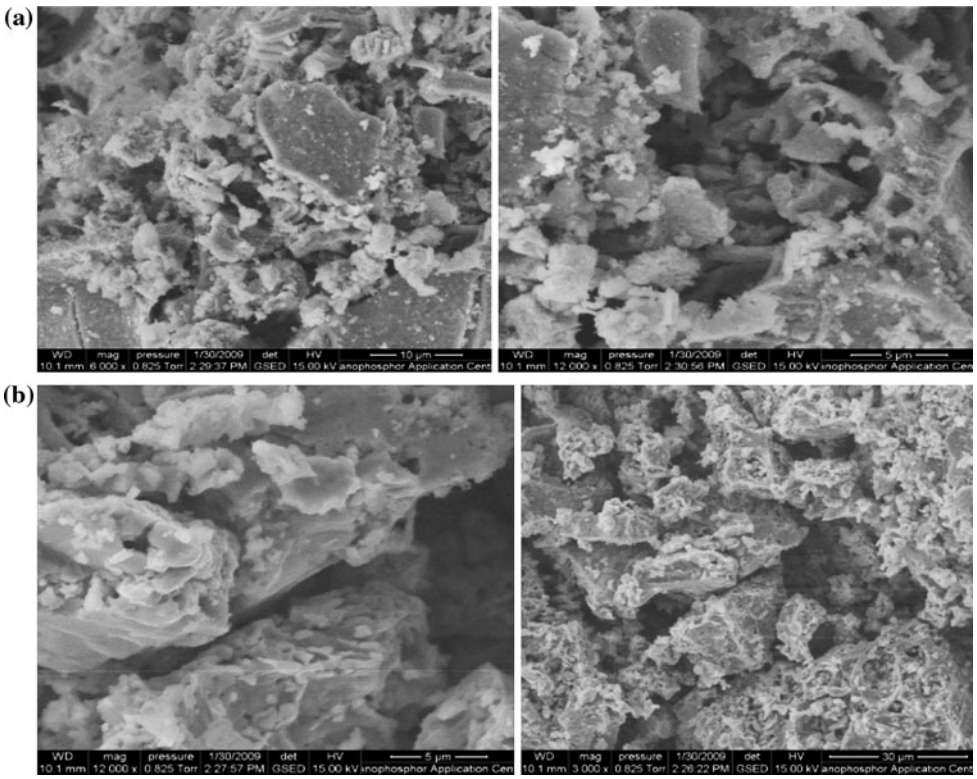

Fig. 5 SEM images of the particles obtained upon annealing at **a** 650 °C and **b** 973 °C

the recording applications. But in most of the hard ferrite applications, the coercivity is >1,500 Oe [34]. Here, the coercivity value is large in case of the product obtained at the low temperature of 450 °C. This may be assigned as a feature of low temperature synthesis of ferrite nanoparticles.

The photoluminescence study of the ferrite nanoparticles were studied using 225, 330, and 350 nm excitation wavelength source. The spectra were found in visible region and these were independent of the particle size. The photoluminescence spectra of these nano-materials are shown in Fig. 7.

The Photoluminescence intensity was found slightly higher in the sample annealed at 650 and 973 °C. The most prominent peaks in visible region were three which is dependent on the particle size. It is well known that color of glasses shows the phenomenon of absorption in the visible spectra. The color due to the fluorescence is shown by the electronic transition with an emission of a photon in the visible region. Photoluminescence is an important phenomenon in which the emission of light takes place from a material under optical excitation. If light of sufficient energy is incident on a material, photons are absorbed leading to electronic excitations. These excitations then relax and the electrons return to the ground state. Photoluminescence occurs when the radiative relaxation occurs. Since the excitation wavelength may influence the photoluminescence of any material, the absorption of a material

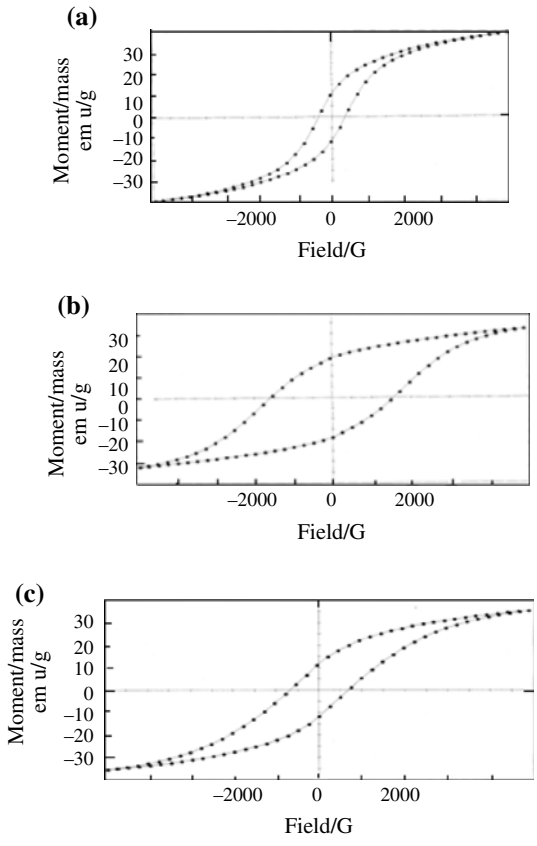

Fig. 6 Magnetic hysteresis curves of $CoFe_2O_4$ nanoparticles obtained upon annealing at **a** 450 °C, **b** 650 °C, and **c** 973 °C

Table 2 Observed magnetic and particle size parameters of cobalt ferrite nanoparticles formed at different temperatures

Annealing temperature/°C	M_r/ emu g^{-1}	M_s/ emu g^{-1}	H_c/Gauss	Mean particle size/nm
450	11.713	35.529	678.60	25
650	18.705	32.018	1574.4	32
973	11.041	39.032	370.91	43

depends strongly on the energy of the incident light. This makes the selection of the excitation light so critical in any photoluminescence study of material. The excitation wavelength controls the density of photo-excited electrons and holes and this governs the behavior of these carriers. Here, the photoluminescence spectrum of the cobalt ferrite nanoparticles annealed at temperatures 450, 650, and 973 °C have been observed at the excitations at 225, 250, and 330 nm, respectively. The spectrum consists of emission peaks at 400 nm (3.09 eV), 480 nm (2.57 eV), 530 nm (2.33 eV), and 650 nm (1.89 eV). It is also observed that the emission intensity of the peaks depends on the excitation wavelength. Regarding the mechanism of PL, it may be due to quantum confinement. This confinement can be explained in terms of shortening of the super-exchange interaction bond length in the nano-crystalline ferrite materials, which modifies the electronic structure of ferrite or in terms of the presence of the fast non-radiative

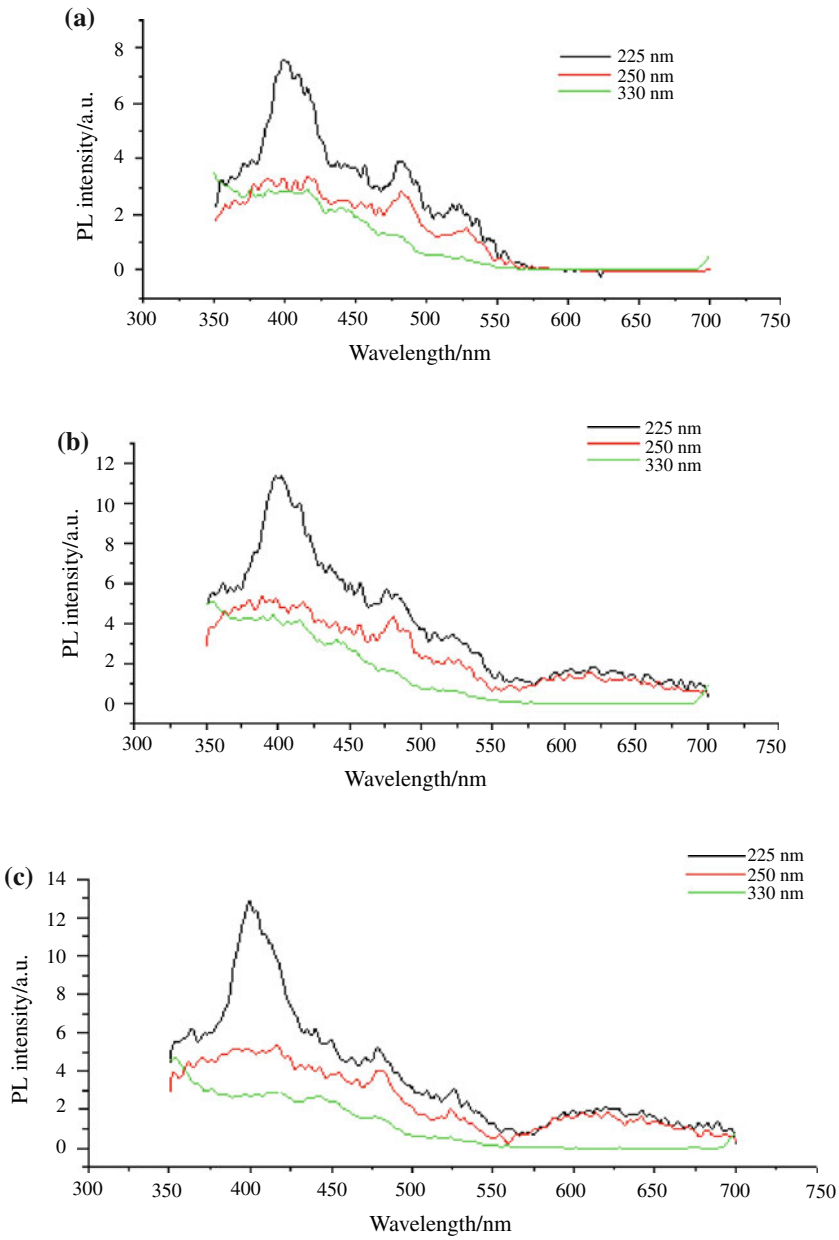

Fig. 7 Photoluminescence Spectra of cobalt ferrite nanoparticles obtained upon annealing at **a** 450 °C, **b** 650 °C, and **c** 973 °C

relaxation channels in nano-crystals which are taking part at the surface. The PL around 3 eV is indeed mainly due to the quantum confinement because the peak value approximately agrees with the band gap of ferrite nanomaterials. The effect of the surface oxide and non-homogenous size is also important if there is a difference in the energies, which is associated with the Stokes shift between the absorption-surface defects or surface oxide. The mechanism of charge transfer between the trivalent ions appears to be involving a nonradiative super-exchange process via the intervening oxide ions that supports the ferromagnetic ordering [35]. The PL has been found to be such that their intrinsic and extrinsic bands were within the visible range [36].

Conclusions

- The TG-DSC curves of the dehydrated gel formed by the coprecipitated iron and cobalt citrates exhibits a clear first step dehydration around 150 °C followed by an *exo* peak which is accompanying the second step. Sample dried below this threshold temperature has a tendency to absorb moisture. Dehydration takes place in the first step of the 5-step decomposition taking place up to 450 °C. After this temperature, only curing is evident and that too in DSC. So, this temperature (450 °C) can be chosen as the minimum temperature for annealing temperature. Annealing was also done at 650 and 973 °C for the sake of comparison.
- The particle size increases with the annealing temperature. The XRD analyses indicated that has a monoclinic unit cell and retentivity and the coercivity values of around 18.7 emu/g and 1574.4 Gauss, respectively, for the $CoFe_2O_4$ nanoparticles obtained upon annealing at 650 °C. The SEM analysis shows individual grains of different shapes as well as few agglomerated grains having different dimensions (0.5–8 μm) are seen in these cases apart from some submicron-sized grains.
- The grain size increases with the increase in temperature of annealing and the grain growth can clearly be seen at 973 °C. Magnetization behavior suggests the possibility of some additional phase at 650 °C. Decrease of M_s implies existence of some phases which can diminish or decrease the M_s and first approximation link goes to existence of some antiferromagnetic phase. Loop of the powders obtained on annealing at 650 °C indicates some hard magnetic materials.
- A size-dependent photoluminescence spectrum of nanoferrite was observed in visible region of different colors only through 250 and 330 nm excitation radiation source.

References

1. Zi Z, Sun Y, Zhu X, Yang Z, Dai J, Song W. Synthesis and magnetic properties of $CoFe_2O_4$ ferrite nanoparticles. J Magn Magn Mater. 2009;321:1251–5.
2. Grigorova M, Blythe HJ, Blaskov V, Rusanov V, Petkov V, Masheva V, Nihtianova D, Martinez LM, Munoz JS, Mikhov M. Magnetic properties and Mössbauer spectra of nanosized $CoFe_2O_4$ powders. J Magn Magn Mater. 1998;183:163–72.
3. Shenker H. Magnetic anisotropy of cobalt ferrite ($Co_{1.01}Fe_{2.00}O_{3.62}$) and nickel cobalt ferrite ($Ni_{0.72}Fe_{0.20}Co_{0.08}Fe_2O_4$). Phys Rev. 1957;107:1246–9.
4. West AR. Basic solid state chemistry. Delhi: Wiley; 1998. p. 356.
5. Salunkhe AB, Khot VM, Phadatare MR, Pawar SH. Combustion synthesis of cobalt ferrite nanoparticles—influence of fuel to oxidizer ratio. J Alloy Compd. 2012;514:91–6.
6. Maaz K, Mumtaz A, Hasnain SK, Ceylan A. Synthesis and magnetic properties of cobalt ferrite ($CoFe_2O_4$) nanoparticles prepared by wet chemical route. J Magn Magn Mater. 2007;308:289–95.
7. Naidek KP, Bianconi F, Rizuti da Rocha TC, Zanchet D, Bonacin JA, Novak MA, Vaz MGF, Winnischofer H. Structure and morphology of spinel MFe_2O_4 (M = Fe, Co., Ni) nanoparticles chemically synthesized from heterometallic complexes. J Colloid Interface Sci. 2011;358:39–46.
8. Cedeno-Mattei Y, Perales-Perez O. Synthesis of high-coercivity cobalt ferrite nanocrystals. Microelectron J. 2009;40:673–6.
9. Fannin PC, Marin CN, Malaescu I, Stefu N, Vlazan P, Novaconi S, Sfirloaga P, Popescu S, Couper C. Microwave absorbent properties of nanosized cobalt ferrite powders prepared by coprecipitation and subjected to different temperature treatments. Mater Des. 2011;32:1600–4.
10. Zhang Y, Yang Z, Yin D, Liu Y, Fei C, Xiong R, Shi J, Yan G. Composition and magnetic properties of cobalt ferrite nano-particles prepared by the co-precipitation method. J Magn Magn Mater. 2010;322:3470–5.
11. Sajjia M, Oubaha M, Prescott T, Olabi AG. Development of cobalt ferrite powder preparation employing the sol–gel technique and its structural characterization. J Alloy Compd. 2010;506:400–6.
12. Verma RK, Hill JO, Niinisto L, Mojumdar SC, Kumar DD. A curriculum framework for education in thermal analysis. J Mater Educ. 2012;34:133–50.
13. Verma RK, Verma L, Chandra M. Thermoanalytical studies on the non-isothermal dehydration and decomposition of dl-lactates of a series of transition metals. Indian J Chem. 2003;42A:2982–7.
14. Bhattacharjee NC, Kumar M, Kumar S, Verma RK. Kinetic and mechanistic studies on non-isothermal decomposition of potassium dioxalatocuprate(II) dihydrate. J Indian Chem Soc. 1998;75(5):317–8.
15. Verma RK, Verma L, Chandra M, Bhushan A. Non-isothermal dehydration and decomposition of dl-lactates of transition metals and alkaline earth metals: a comparative study. J Therm Anal Calorim. 2005;80:351–4.
16. Kumar M, Verma RK, Verma L, Bhattacharjee NC, Kumar S, Verma BP. Thermal decomposition of potassium trioxalato chromate(III) trihydrate: a kinetic and mechanistic study. Asian J Chem. 1996;8(3):543–6.
17. Agrawal HL, Mishra A, Ambasta RK, Verma L, Verma RK, Verma BP. Kinetic parameters of thermolysis of complexes of rhodium(III), palladium(II) and platinum(II) with substituted morpholines from their non-isothermal thermogravimetric data. Asian J Chem. 1994;6:130–4.
18. Verma BP, Verma RK, Chandra M, Pandey S, Mallick AK, Verma L. A study of non-isothermal decomposition of calcium dl-lactate pentahydrate. Asian J Chem. 1994;6:606–12.

19. Verma RK, Verma L, Ranjan M, Verma BP, Mojumdar SC. Thermal analysis of 2-oxocyclopentanedithiocarboxylato complexes of iron(III), copper(II) and zinc(II) containing pyridine or morpholine as the second ligand. J Therm Anal Calorim. 2008;94:27–31.
20. Verma RK, Verma L, Bhushan A, Verma BP. Thermal decomposition of complexes of cadmium(II) and mercury(II) with triphenylphosphanes. J Therm Anal Calorim. 2007;90:725–9.
21. Brown ME, Gallagher PK. Introduction to recent advances, techniques and applications of thermal analysis and Calorimetry. In Brown ME, Gallagher PK, Editors. Hand book of thermal analysis and calorimetry. Elsevier: New York; 2008. pp. 1–12.
22. Verma RK, Verma L, Chandra M, Verma BP. Kinetic parameters of thermal dehydration and decomposition from thermoanalytical curves of zinc dl-lactate. J Indian Chem Soc. 1998;75:162–4.
23. Singh RK, Yadav A, Narayan A, Singh AK, Verma L, Verma RK. Thermal, structural and magnetic studies on chromite spinel, synthesized by citrate precursor method and annealed at temperature 450 °C and 650 °C. J Therm Anal Calorim. 2012;107:197–204.
24. Singh RK, Yadav A, Narayan A, Chandra M, Verma RK. Thermal, XRD and magnetization studies on $ZnAl_2O_4$ and $NiAl_2O_4$ spinels, synthesized by citrate precursor method and annealed at temperature 450°C and 650°C. J Therm Anal Calorim. 2012;107:205–10.
25. Goldstein AN (ed.), Handbook of nanophase materials. New York: Marcel Dekker; 1997. p. 1.
26. Panda RN, et al. Magnetic properties of nano-crystalline Gd or Pr substituted $CoFe_2O_4$ synthesized by the citrate precursor technique. J Magn Magn Mater. 2003;257:79–86.
27. Sajjia M, Benyounis KY, Olabi AG. The simulation and optimization of heat treatment of cobalt ferrite nanoparticles prepared by sol–gel technique. Powder Technol. 2012;222:143–51.
28. Cullity BD. Elements of X-ray diffraction. New York: Wiley; 1978. p. 101.
29. Roisnel J, Rodrıguez-Carvajal J, WinPLOTR; Laboratoire Leon Brillouin (CEA-CNRS) Centre d'Etudes de Saclay: Gif sur Yvette Cedex, France, 2000.
30. Rodriguez-Carvajal J. FullProf 2000: A Rietveld Refinement and Pattern Matching Analysis Program, (Version: April 2008), Laboratoire Léon Brillouin (CEA-CNRS), France.
31. Williamson GK, Hall WH. X-ray line broadening from filed aluminium and wolfram. Acta Metal. 1953;1:22.
32. Bhowmik RN. Lattice expansion and magnetic order in spinel oxide. Kolkata: Proceedings of National Conference on Nanoscience & Nanotechnology; 2009.
33. Chinnasamy CN, Jeyadevan B, Perales-Perez O, Shinoda K, Tohji K, Kasuya A. Growth dominant co-precipitation process to achieve high coercivity at room temperature in $CoFe_2O_4$ nanoparticles. IEEE Trans Magn. 2002;38(5):2640–2.
34. Bahadur D. Current trends in applications of magnetic ceramic materials. Bull Mater Sci. 1992;15(5):431–9.
35. Bandyopadhay AK. Nanomaterials. New. Delhi: New age international; 2007. pp. 254–267.
36. Xi YY, Cheung TLY, Dickon HLN. Synthesis of ternary $Zn_xCd_{1-x}S$ nanowires by thermal evaporation and the study of their photoluminescence. Mater Lett. 2008;62:128–32.